Identification of the Number of Overlapping Welded Thin Plates in an X-ray CT Volume

Naoya Sakabe , Yutaka Ohtake , Yukie Nagai , Hiromasa Suzuki

The University of Tokyo,
{ sakabe, ohtake, yukie, suzuki } @den.t.u-tokyo.ac.jp

Corresponding author: Naoya Sakabe, sakabe@den.t.u-tokyo.ac.jp

Abstract. Currently, optical 3-D scanners are used to reverse engineer vehicle chassis. Complete reverse engineering using optical scanners requires dismantling the samples. Therefore, industrial X-ray CT scanners must be used to enable a non destructive and time efficient process. We suggest a new method to segment CT volumes into regions with the same number of overlapping thin plates. By calculating the gradients on every surface voxel and searching for the other side of the surface, thickness values can be assigned to all surface voxels. Applying the multilabel graph cut algorithm, volumes are segmented into regions. The effectiveness of our method is demonstrated via experiments on two chassis samples.

Keywords: X-ray CT, reverse engineering, thin plates, segmentation
DOI: https://doi.org/10.14733/cadaps.2019.318-328

1 INTRODUCTION

1.1 Background

Research and development of vehicles demand internal inspection of the chassis parts that are assembled at other companies; this is called reverse engineering.

Reverse engineering is accelerated by digitizing the surface and internal shapes of parts. Optical 3-D scanners are often used nowadays for this purpose [7]. Optical scanners cannot inspect the internal shape of assembled parts; thus, users have to dismantle such parts. Applying an industrial X-ray CT in such cases would be useful because it facilitates non destructive, time-efficient digitization of assembled parts [3].

© 2019 CAD Solutions, LLC, http://www.cad-journal.net

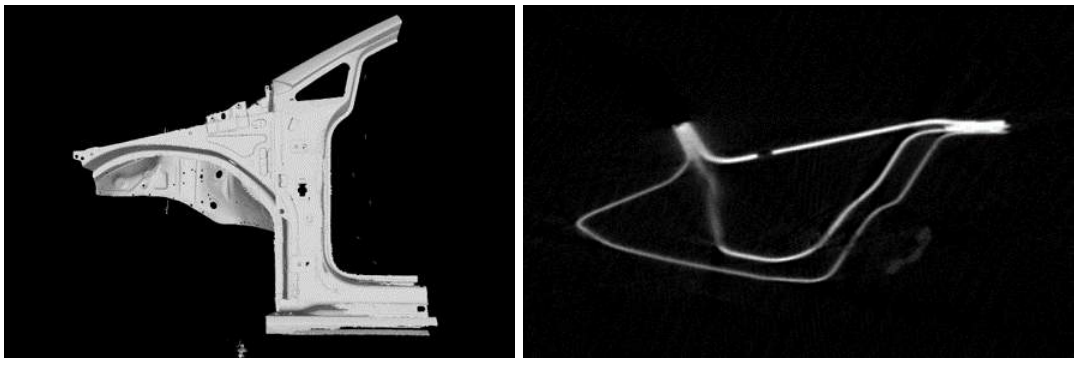

Figure 1: A vehicle's CT volume including welding spots and one of its slices.

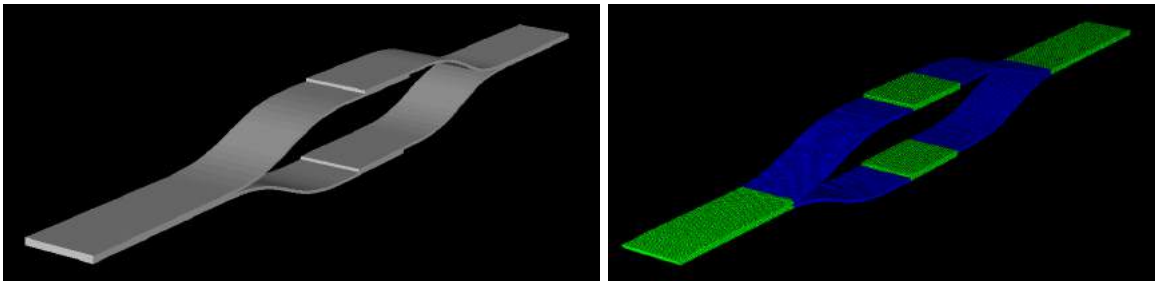

Figure 2: A simple example of overlapping plates and the processing result.

1.2 Problem of Welded Parts in an X-ray volume

A 3-D X-ray CT volume represents the distribution of the attenuation coefficient in 3-D space. Attenuation coefficients are determined by the material's density; therefore, parts with different materials can be distinguished by thresholding the CT value.

However, in our situation, vehicle chassis almost always consists of single material (Figure 1). Welded metal parts with the same material are contiguous on CT volume. Simple thresholding is not sufficient to segment parts.

1.3 Research Goals

To support the reverse engineering of vehicle chassis, we aim to provide information on the number of thin plates, particularly in the near field of welding spots. The information can be visualized by coloring the CT volume or by extracting the regions which have the same number of plates overlapping. Figure 2 shows overlapping thin plates and the result of our computation. In the right image in Figure 2, regions with overlap are distinguished and appear green, whereas non overlapping regions appear blue.

1.4 Related Research

A method was previously proposed to extract medial surfaces from a CT volume, including welded plates, based on searching medial cells and classifying and editing them [5]. These steps restrict the method to process no

© 2019 CAD Solutions, LLC, http://www.cad-journal.net

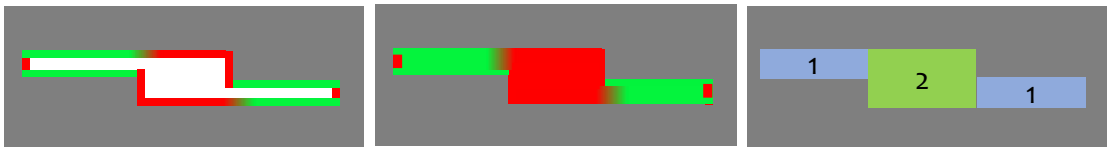

(a) Surface voxels have a thickness value (b) Foreground voxels have a thickness value (c) Regions labeled by the number of thin plates

Figure 3: Simplified illustration of the computed results.

more than two thin plates.

The proposed method enables treating more than three plates. This leads to a more efficient and useful reverse engineering process.

2 ALGORITHM

Our algorithm considers and provides the following inputs/outputs.
Inputs:

- A 3-D X-ray CT volume containing the vehicle chassis
- A threshold value between the material and the air
- The thickness of the metal plates in the pressed part

Outputs:

- A 3-D point set with the thickness values.
- A 3-D point set with the number-of-plate labels.

Our algorithm can be briefly explained as follows. A simplified expression of a volume is shown in Figure 3.

1. The surface voxels on the CT volume are defined.
2. The thickness of the part on each surface voxel is calculated (Figure 3a).
3. The thickness values are propagated into the inner voxels (Figure 3b).
4. The number of plates on each foreground voxel are determined according to the thickness value (Figure 3c).

In the step 1, the CT volume is binarized using the input threshold value, and it defines surface voxels on the boundaries. Next, in the step 2, thickness values for each surface voxels are caluculated by searching another one.

After that, we have thickness values only on the surface voxels. We want a solid region of the metal parts. So in the step 3, we propagate the values on the surface into the inner region. Then, we operate the graph cut optimization to segment the solid volume.

As assumptions, the following conditions are applied.

- The thicknesses of thin plates in the CT volume are the same.
- The thickness of the thin plates is approximately several times over the voxel size.

The sections below explain detailed procedures.

© 2019 CAD Solutions, LLC, http://www.cad-journal.net

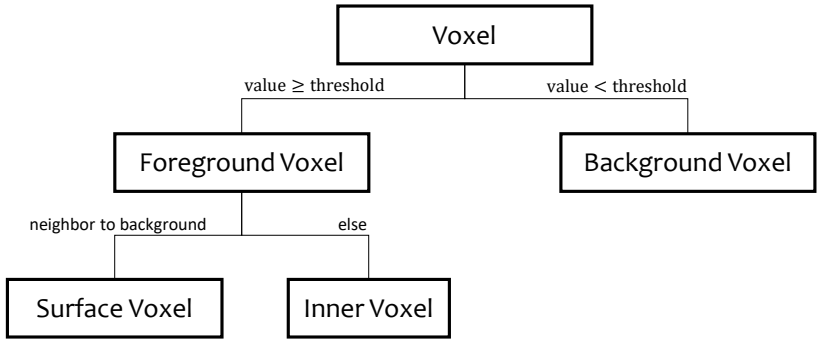

Figure 4: Attributes of the Voxels

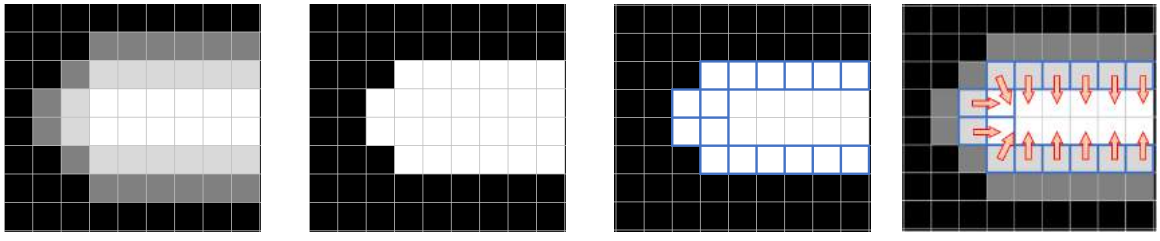

(a) CT volume (b) Binarized by thresholding (c) Defined surface voxels (d) Gradient vectors

Figure 5: Steps to calculate the gradient vectors on the CT volume.

2.1 Attributes of the Voxels

The attributes for the voxels are defined, as shown in Figure 4.

Voxels are of two types: foreground and background. These attributes are determined by thresholding. Foreground voxels branch into surface and inner voxels. We explain this further in Section 2.2.

2.2 Definition of Surface Voxels

To begin calculating the thickness of the CT volume, we define surface voxels on the boundary of metal and air (Figure 5). Note that Figure 5 is a simplified example in a 2-D representation.

Starting from a CT volume (Figure 5(a)), for each voxel, we determine if the voxel is a foreground voxel (the value is above the threshold) or a background voxel (the value is below the threshold). This procedure is called binarization. The result is shown in Figure 5(b).

Next, we define the surface voxels by the following condition: surface voxels are foreground voxels that have at least one background voxel among their 26 neighboring voxels. Other foreground voxels, other than surface voxels, are marked as inner voxels. In Figure 5(c), surface voxels are marked with a blue border.

2.3 Measurement of Distance

In this step, we calculate the thickness value for each surface voxel. By searching another surface voxel, we can define an approximate thickness on voxel-level. Moreover, to achieve sub-voxel-level precision, detailed calculations are applied on the value.

© 2019 CAD Solutions, LLC, http://www.cad-journal.net

For each surface voxel p_1, we search for another surface voxel p_2 in the direction of the gradient $G = \nabla I$, where I represents the intensity value of the CT volume. These vectors are shown as red arrows in Figure 5(d). The distance between these two voxels represents the approximate (voxel-level) thickness of the chassis.

To achieve sub-voxel-level measurement, we suggest refinement. First, we define the penetration L as a straight line passing through the voxels p_1 and p_2 as shown in Figure 6. Then, we interpolate the gradient field I on the penetration L via trilinear interpolation. We denote this as $\nabla I(x)$, where x is the coordinate on the straight line L. Taking the inner product $\nabla I(p_1) \cdot \nabla I(x)$, we obtain a function, such as that shown in Figure 7. The argument of the maximum and minimum of the function will be found near p_1 and p_2. By defining the argument of the maximum and minimum of $\nabla I(p_1) \cdot \nabla I(x)$ as the new boundaries of this plate, we obtain a fine measurement T_{p_1} of the thickness of the plate.

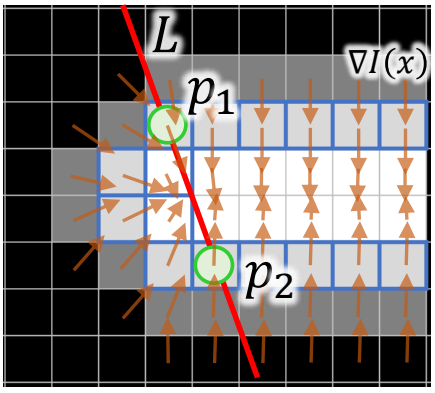

Figure 6: Definition of the penetration L based on the voxels p_1 and p_2.

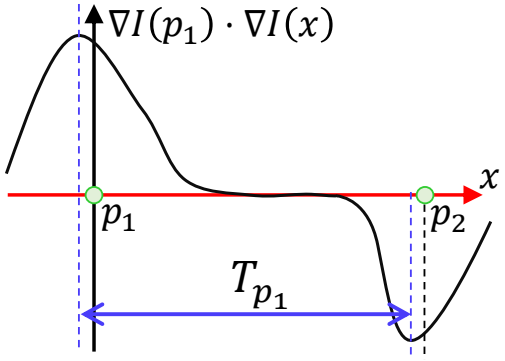

Figure 7: Fine definition of the boundaries and the measurement T_{p_1}

2.4 Propagating Values into Inner Voxels

Now, we have the surface voxels and their calculated thickness values. In the segmentation of the volume, it is preferred that all *foreground* voxels have some value. In this step, we assign a value to the *inner* voxels, which have no value so far.

We want the inner voxels to have a value close to the nearest *surface* voxel. To achieve this, the following process is applied.
For each inner voxel p,

1. Enumerate the voxels that already have a value among the 26-neighboring voxels; and
2. Set the median value of these (enumerated) voxels as the value of p.

This process is iterated until no voxels are modified. After finishing this process, nearly all foreground voxels will have some value representing the thickness around them.

26-neighboring voxels are the voxels which share at least one vertex with p. The concept of 26-neighboring voxels is illustrated in Figure 8b, contrasted with that of 6-neighboring (Figure 8a).

2.5 Determining the Number of Plates

Let us consider a method to label the foreground voxels with the number of thin plates. It is too complex to calculate all the combinations of voxels with all labels (such as 1, 2, 3, ...). Therefore, we adopted the multi

© 2019 CAD Solutions, LLC, http://www.cad-journal.net

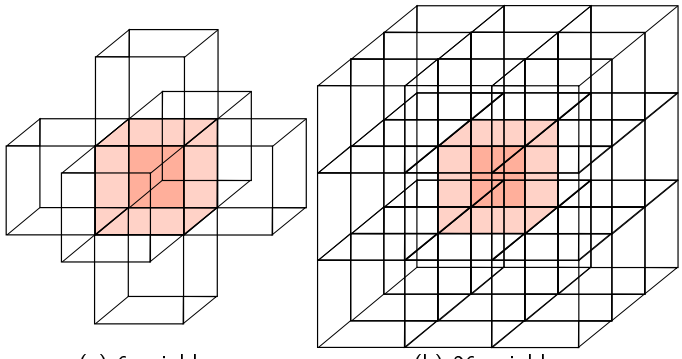

(a) 6 neighbors (b) 26 neighbors

Figure 8: Illustration of 6- and 26-neighboring voxels.

label graph cut algorithm, which can segment a graph into partial graphs with some labels [1][2][6][4].

The graph cut algorithm yields an optimized segmentation that minimizes an energy function E, which is denoted as

$$E(f) = \sum_{l \in \mathcal{L}} \sum_{p:f_p=l} D\left(T_p, l\right) + \lambda \sum_{pq \in \mathcal{N}} [f_p \neq f_q] + \sum_{l \in \mathcal{L}} h_l \cdot \delta_l(f). \tag{1}$$

Here, p is the voxel of interest, f is a labeling pattern and l is a label $(l = 1, 2, \ldots)$. T_p is the value of thickness of the voxel p. $\mathcal{L}$ is a set of labels. $\mathcal{N}$ is a set of pairs of neighboring voxels. $[f_p \neq f_q]$ yields 1 if $f_p \neq f_q$ is established, otherwise it yields 0. The definition of δ_l is

$$\delta_l(f) = \begin{cases} 1 & \exists p \,:\, f_p = l \\ 0 & \text{otherwise.} \end{cases} \tag{2}$$

Some expressions have been altered from those of Ref. [4].

The first term of Eq. (1) is called the data cost. This term provides a low value when the thickness value T_p likely to appear in the label l. For our problem, we use "l-plateness" for the data cost function and define it as

$$D(T_p, l) = \frac{2(T_p - lt)^2}{t^2}.$$

The second term in Eq. (1) is called the smooth cost. This term is low when the labeling boundaries are smooth. The weight of the smooth cost is determined by the parameter λ. The last term in Eq. (1) adds energy when more labels are used.

The two coefficients, λ and h_l, need to be specified by the user.

3 EXPERIMENTS

3.1 Environments

The computer used in these experiments was equipped with Intel Xeon E5-2667 v4 3.20 GHz, 256 GB of RAM and Windows 10 Pro version 1709. Volume rendering images were provided by Avizo 9.4.0. Colored images were rendered using MeshLab v2016.12.

© 2019 CAD Solutions, LLC, http://www.cad-journal.net

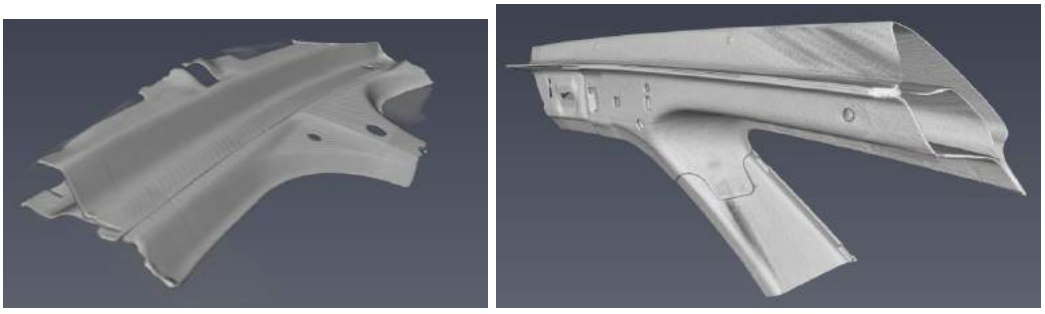

(a) Sample A (b) Sample B

Figure 9: Volume rendering images of two samples.

3.2 Samples

The two samples used in our experiments are shown in Figure 9.

Sample A is part of a vehicle chassis. It includes several welding spots and an overlapping area of two plates at its center. The approximate thickness of a single thin plate is $1.0\,\mathrm{mm}$. The calculation time was approximately 2 min.

Sample B is also part of a vehicle chassis. It contains more complicated welding shapes and overlapping areas with three plates. The approximate thickness of a single thin plate is $1.5\,\mathrm{mm}$. The calculation time was approximately 20 min.

3.3 Parameters Searching

Firstly, we conducted parameter searching using Sample A. There are two floating parameters, the smooth cost λ and the label cost h_l. We estimated the order of the parameters λ and h_l by combining the values and functions, $\lambda \in \{1, 10, 100, 1000\}$ and $h_l \in \{0, 10^l, 10^{2l}\}$. See Fig. 10. There seems to be nothing to do with the label cost h_l. On the other hand, the smooth cost λ has a significant effect on the segmentation result. In the case $\lambda = 1$, too much separation was applied. Conversely, there are no region that has been identified to be overlapping in the case $\lambda = 1000$. We adopt $\lambda = 10, h_l = 10^l$ as the parameters of following experiments.

3.4 Results

The results of identification for sample A are shown in Figure 11. The overlapping area at the center of the images is properly colored as a two-plate region. The other areas without welding are colored as single-plate regions.

The results for sample B are shown in Figure 12. The welded region with three thin plates on the upper half of the left column is properly colored red. Areas with two plates are colored green.

4 CONCLUSIONS

We succeeded in calculating the thickness of two 3-D CT volumes and segmented them into regions labeled by the number of thin plates. This type of imaging can lead to a more detailed analysis of the assembled vehicle parts.

© 2019 CAD Solutions, LLC, http://www.cad-journal.net

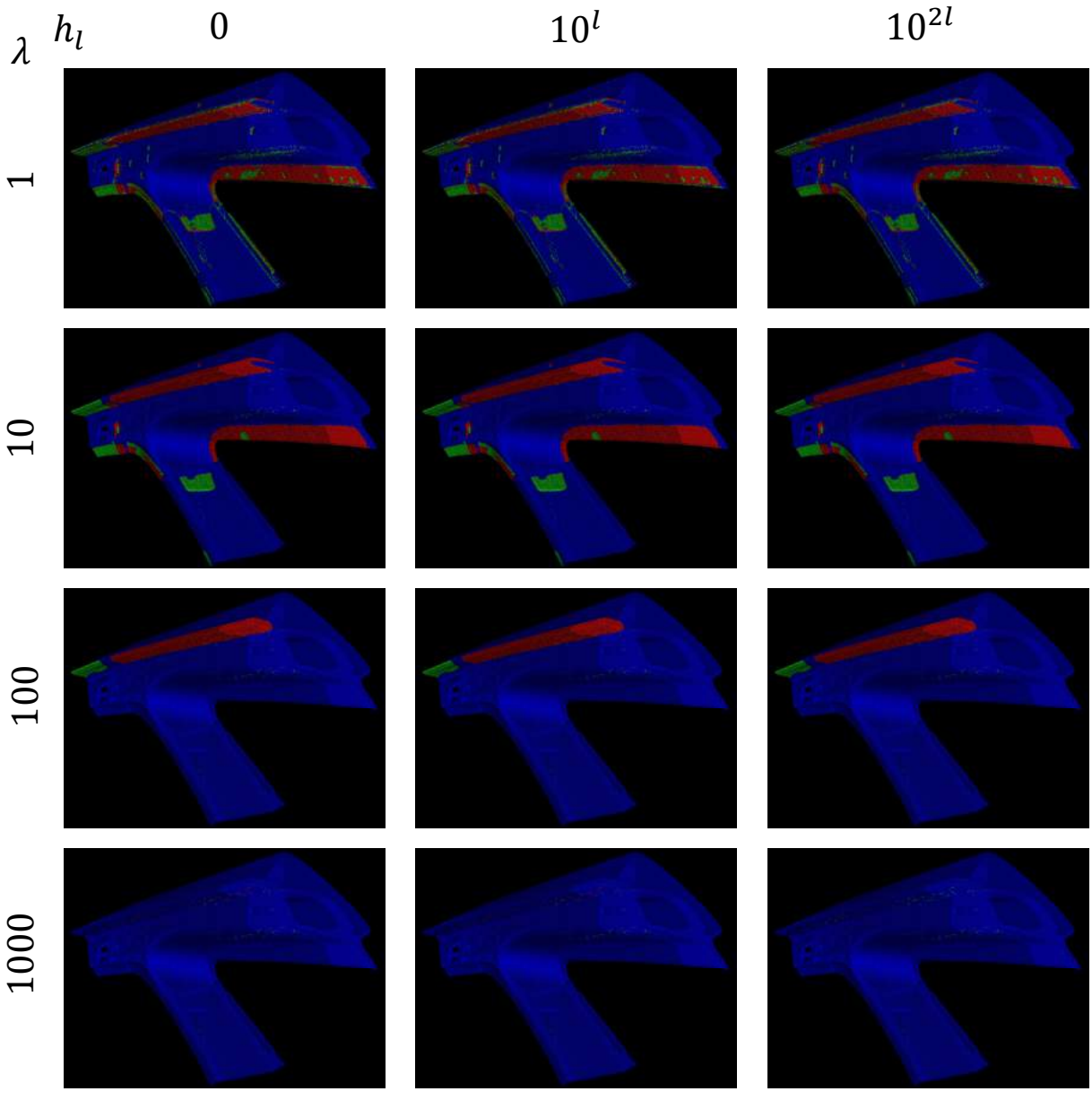

Figure 10: Results of parameter searching.

© 2019 CAD Solutions, LLC, http://www.cad-journal.net

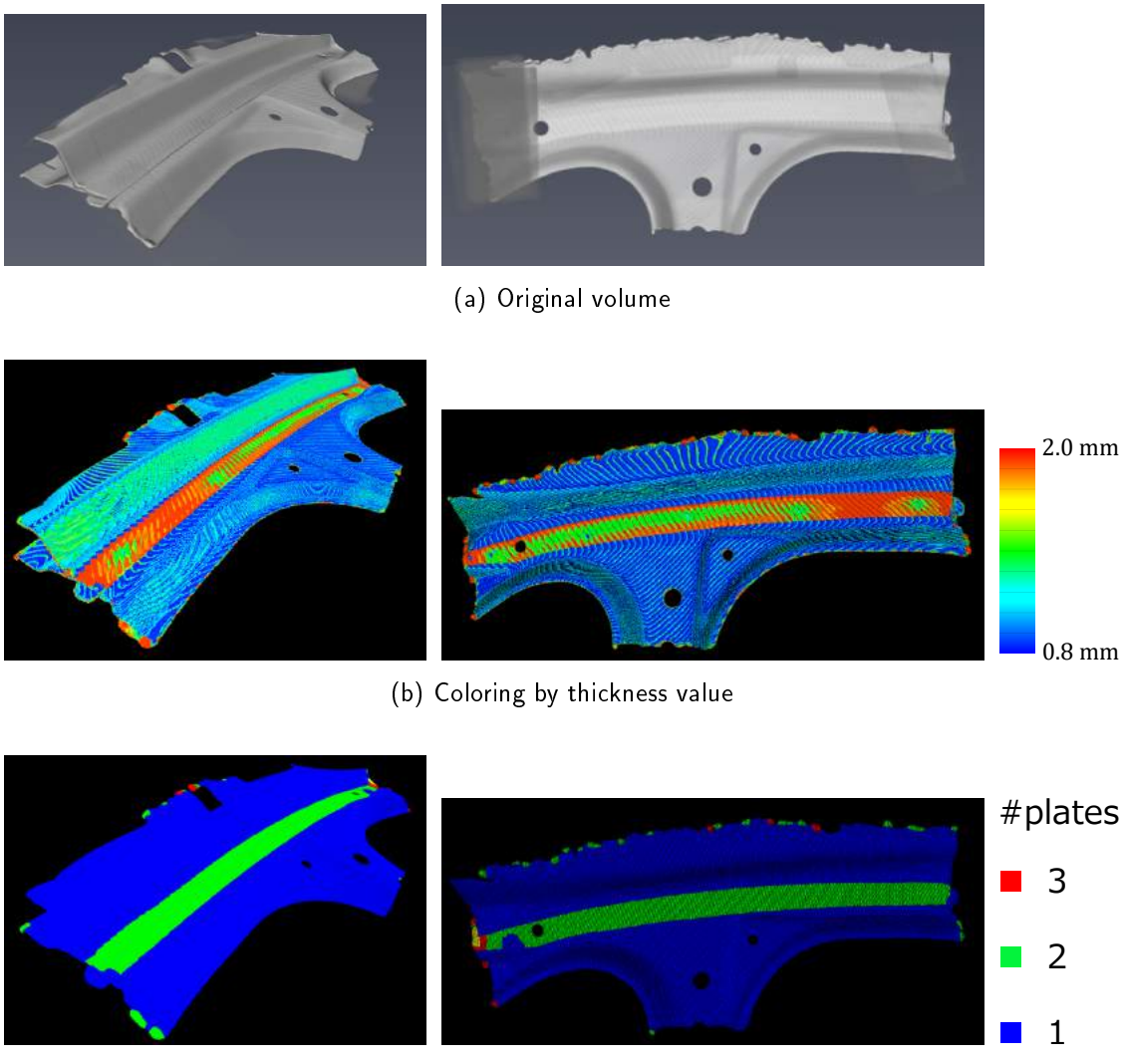

(a) Original volume

(b) Coloring by thickness value

(c) Coloring by segmented label

Figure 11: Results for Sample A.

© 2019 CAD Solutions, LLC, http://www.cad-journal.net

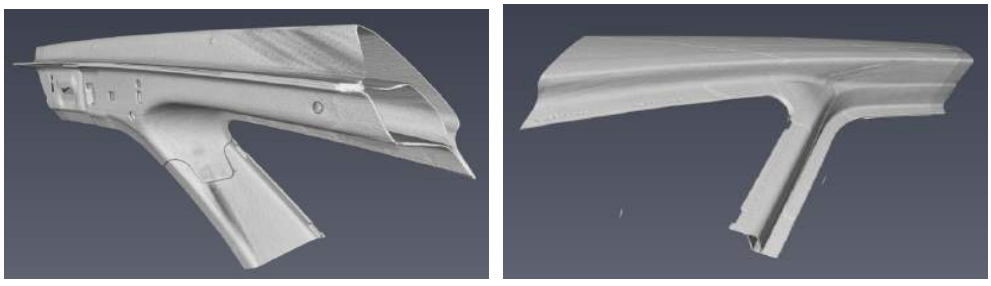

(a) Original volume

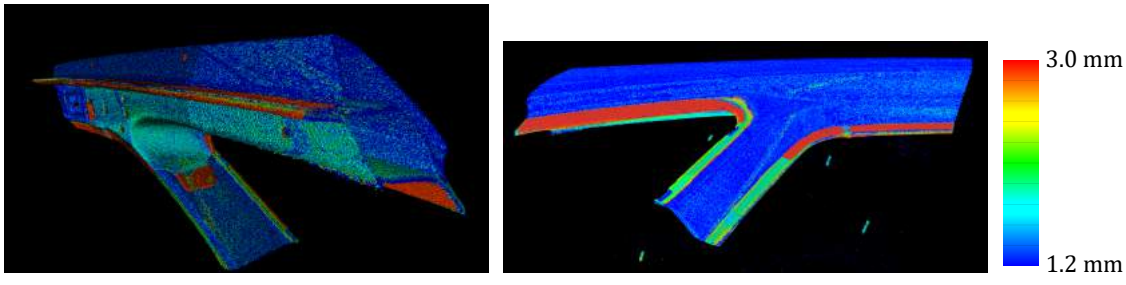

(b) Coloring by thickness value

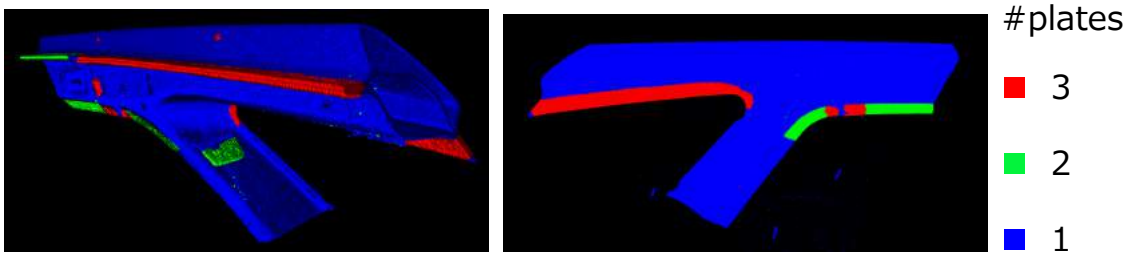

(c) Coloring by segmented label

Figure 12: Results for Sample B.

© 2019 CAD Solutions, LLC, http://www.cad-journal.net

For example, we could extract the CAD surfaces of each thin plate. Using the number of plates and the contiguity of the regions would make this possible. The extracted CAD surfaces would give us useful hints for the reverse engineering process.

The thickness data for the volumes will also be useful for other types of analyses, for example, weld spot detection. Significant features around welding spots can be detected by analyzing our data. Information of weld spot is also helpful when treating the CT volumes of vehicles.

ACKNOWLEDGEMENTS

A part of CT volumes, Figure 1 and Sample B, is courtesy of G-TEKT Corporation.

ORCID

Naoya Sakabe http://orcid.org/0000-0001-9458-8906
Yutaka Ohtake http://orcid.org/0000-0002-1368-9172
Yukie Nagai http://orcid.org/0000-0002-7362-2703
Hiromasa Suzuki http://orcid.org/0000-0003-4237-1101

REFERENCES

[1] Boykov, Y.; Kolmogorov, V.: An experimental comparison of min-cut/max- flow algorithms for energy minimization in vision. IEEE Transactions on Pattern Analysis and Machine Intelligence, 26(9), 1124–1137, 2004. ISSN 0162-8828. http://doi.org/10.1109/TPAMI.2004.60.

[2] Boykov, Y.; Veksler R., O.; Zabih, R.: Efficient approximate energy minimization via graph cuts. IEEE Transactions on Pattern Analysis and Machine Intelligence, 20(12), 2001.

[3] Chiffre, L.D.; Carmignato, S.; Kruth, J.P.; Schmitt, R.; Weckenmann, A.: Industrial applications of computed tomography. CIRP Annals, 63(2), 655 – 677, 2014. ISSN 0007-8506. http://doi.org/10.1016/j.cirp.2014.05.011.

[4] Delong, A.; Osokin, A.; Isack, H.N.; Boykov, Y.: Fast approximate energy minimization with label costs. International Journal of Computer Vision, 96(1), 1–27, 2012. ISSN 1573-1405. http://doi.org/10.1007/s11263-011-0437-z.

[5] Fujimori, T.; Kobayashi, Y.; Suzuki, H.: Separated medial surface extraction from ct data of machine parts. In M.S. Kim; K. Shimada, eds., Geometric Modeling and Processing - GMP 2006, 313–324. Springer Berlin Heidelberg, Berlin, Heidelberg, 2006. ISBN 978-3-540-36865-6.

[6] Kolmogorov, V.; Zabin, R.: What energy functions can be minimized via graph cuts? IEEE Transactions on Pattern Analysis and Machine Intelligence, 26(2), 147–159, 2004. ISSN 0162-8828. http://doi.org/10.1109/TPAMI.2004.1262177.

[7] Sansoni, G.; Docchio, F.: In-field performance of an optical digitizer for the reverse engineering of free-form surfaces. The International Journal of Advanced Manufacturing Technology, 26(11), 1353–1361, 2005. ISSN 1433-3015. http://doi.org/10.1007/s00170-004-2122-7.

© 2019 CAD Solutions, LLC, http://www.cad-journal.net